Optical patterns in spatially coupled phase-conjugate systems*

Yue Li-Juan(岳立娟)† and Sang Jin-Yu(桑金玉)

College of Physics, Northeast Normal University, Changchun 130024, *China*

(Received 19 January 2010; revised manuscript received 18 May 2010)

Various pattern evolutions are presented in one- and two-dimensional spatially coupled phase-conjugate systems (SCPCSs). As the system parameters change, different patterns are obtained from the period-doubling of kink–antikinks in space to the spatiotemporal chaos in a one-dimensional SCPCS. The homogeneous symmetric states induce symmetry breaking from the four corners and the boundaries, finally leading to spatiotemporal chaos with the increase of the iteration time in a two-dimensional SCPCS. Numerical simulations are very helpful for understanding the complex optical phenomena.

Keywords: pattern evolution, phase-conjugate, one- and two-dimensional spatially systems
PACC: 0545

1. Introduction

The characterisation of complex phenomena has been studied mainly within a scope of nonlinear sciences. There are multiple stable and unstable states in high-dimensional systems. So high-dimensional systems have more complicated behaviours and more abundant characteristics. The potential application is extremely significant. The formation of patterns is a common feature in many physical processes. In the far-from-equilibrium regime, the evolutions of patterns are studied, not only in fluid dynamics but also in solid-state physics, optics, chemical reaction with diffusion, and biology. In the study of high-dimensional chaotic systems, coupled map lattices have played an important role in being paradigms for a wide variety of fascinating phenomena.[1−13] Recently, it was found that many coupled map lattices shared a common sequence of patterns, no matter whether local maps are different.[14,15] Although the nonlinear optic phenomena of the phase conjugate resonators were studied,[16−21] the pattern formation and spatiotemporal chaos in the spatially coupled phase-conjugate systems (SCPCS) have not been reported. In the present paper, various patterns are presented from the period-doubling of kink–antikinks in space and the chaotic behaviours in some domains to the spatiotemporal chaos with the increase of the system parameter in a one-dimensional SCPCS. The homogeneous symmetric states induce symmetry breaking from four corners and the boundaries, finally leading to spatiotemporal chaos with the increase of the iteration time in a two-dimensional SCPCS. These results are very helpful for understanding the complicated optical phenomena. They have important potential application in processing information and transmitting information.

2. Theoretical model

The phase-conjugate resonator consists of one normal mirror and one phase-conjugate mirror (PCM). The schematic diagram of the phase-conjugate resonator is shown in Fig. 1.

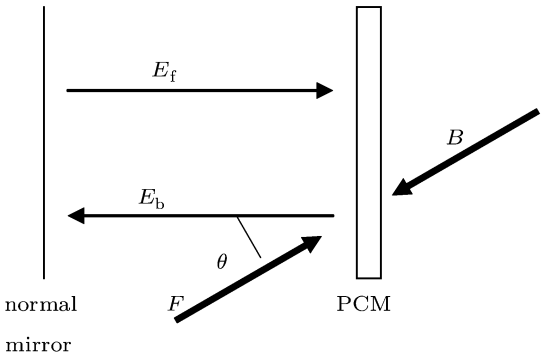


Fig. 1. Schematic diagram of the phase-conjugate resonator.

*Project supported by the National Natural Science Foundation of China (Grant No. 10847110).
†Corresponding author. E-mail: ljyue@nenu.edu.cn
© 2010 Chinese Physical Society and IOP Publishing Ltd

The conjugator is assumed to be a lossless Kerr medium treated in the Raman–Nath approximation. Multiple scattering orders are possible. The normal mirror is so positioned that only the zeroth- or the first-order scattered light can return. The zeroth-order scattered light is given by[19]

$$E_{\rm b} = ZB{\rm J}_0(2\,|FE_{\rm f}^*|). \tag{1a}$$

The first-order scattered light is

$$E_{\rm b} = {\rm i}\,ZB{\rm J}_1(2\,|FE_{\rm f}^*|)FE_{\rm f}^*/\,|FE_{\rm f}|\,, \tag{1b}$$

where $Z = \exp({\rm i}(|F|^2 + |B|^2 + |E_{\rm f}|^2))$ represents a field-dependent phase shift introduced by reflection, $\rm J_0$ and $\rm J_1$ are the standard Bessel functions, and F and B are two laser pumps pumping the medium. We assume that all four beams are plane waves. When the backscattered light $E_{\rm b}$ is fed back into the cavity by the normal mirror, all of the necessary ingredients for dissipative chaos are present. Non-linearity is provided by the medium, and driving can be achieved by the pump and then feedback comes from the normal mirror. The forward-propagating field $E_{\rm f}$ experiences instabilities and is driven to chaos by increasing the pump intensity. The field $E_{\rm f}(t+\tau)$ after one round-trip time is obtained as

$$E_{\rm f}(t+\tau) = [{\rm FSP}][{\rm REFL}][{\rm FSP}]E_{\rm b}(t), \tag{2}$$

where [FSP] denotes the free-space propagation from one mirror to the other, [REFL] represents the reflection operator from the normal mirror. Equations (1) and (2) can be combined into an iterative map of the form.[16] The zeroth-order reflection is given as follows:

$$I_{n+1} = \gamma I_{\rm B}{\rm J}_0^2(2(I_{\rm F}I_n)^{1/2}), \tag{3a}$$

$$\Phi_{n+1} = (2KL + \Phi_{\rm B} + I_{\rm F} + I_{\rm B} + I_n){\rm mod}(2\pi), \tag{3b}$$

and the first-order reflection

$$I_{n+1} = \gamma I_{\rm B}{\rm J}_1^2(2(I_{\rm F}I_n)^{1/2}), \tag{4a}$$

$$\Phi_{n+1} = (2KL + \Phi_{\rm F} + \Phi_{\rm B} + I_{\rm F} + I_{\rm B} + I_n - \Phi_n){\rm mod}(2\pi), \tag{4b}$$

where $I_n = |E_{\rm f}(t+n\tau)|^2$ is the intensity; Φ_n is the phase of the forward field after n round-trips; $I_{\rm F}$, $I_{\rm B}$, $\Phi_{\rm F}$ and $\Phi_{\rm B}$ are the corresponding quantities for the pumps; γ is the intensity reflection coefficient of the normal mirror; $2KL$ is the round-trip phase shift. The intensity is more important in understanding the overall intra-cavity field behaviour. Therefore, we transform the multimodal intensity into the following equation:

$$X_{n+1} = A{\rm J}_{0/1}^2(X_n^{1/2}), \tag{5}$$

which has been obtained from Eqs. (3a) and (4a) by assuming $X_n = 4I_{\rm F}I_n$ and $A = 4\gamma I_{\rm F}I_{\rm B}$. The general form including switch-off or threshold effects is put into the two-parameter equation:

$$X_{n+1} = A{\rm J}_{0/1}^2((X_n - B)^{1/2}), \tag{6}$$

where B is the switch-off parameter. For $x_n < B$ the J-functions change into Bessel I-function. Thus, below B it is possible to have amplification or lasing in the system, which is turned off above B. As for $B = 0$, it returns to Eq. (5). As for $B = 3$, the bifurcation diagram and the maximum Lyapunove exponent spectrum of the first-order reflection are shown in Fig. 2. It is shown that the system varies from period double to chaos at different values of A. Here, in the present paper, we will discuss the first-order reflection.

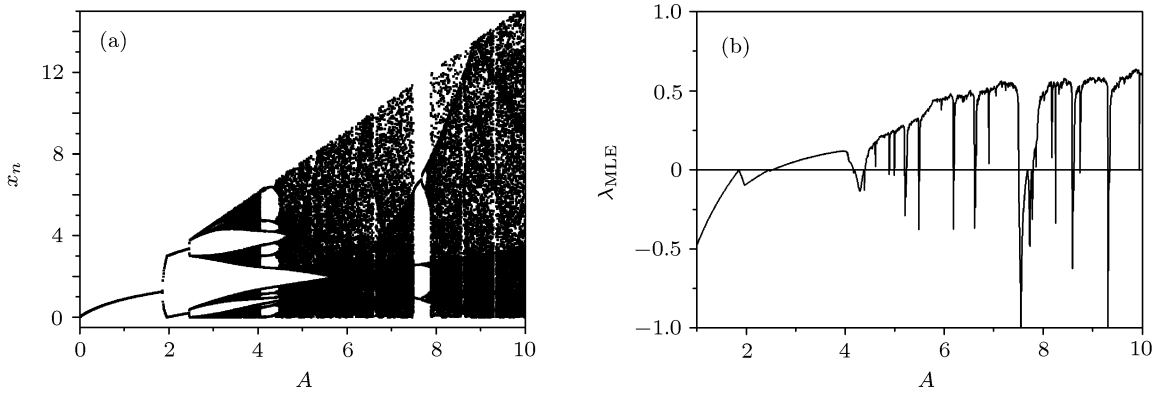


Fig. 2. Switch-off parameter $B = 3$ in expression $X_{n+1} = A{\rm J}_1^2((X_n - B)^{1/2})$. (a) Bifurcation diagram, (b) maximum Lyapunov exponent spectrum.

3. Numerical results

The coupled map lattice (CML) is a dynamical system with a discrete time, discrete space, and continuous state.[1,2] There are many merits for the study of spatiotemporal chaos. In the present paper, the CML is investigated as a model for the SCPCS. The optical patterns have been shown both in the one-dimensional SCPCS and in the two-dimensional SCPCS.

3.1. One-dimensional coupled map phase-conjugate system

One-dimensional CML is in the following general form:[1]

$$x_{n+1}(i) = (1-\varepsilon)f(x_n(i)) + \frac{\varepsilon}{2}(f(x_n(i+1)) + f(x_n(i-1))), \tag{7}$$

where $n = 1, 2, \ldots N$ are discrete time steps; $i = 1, 2, \ldots L$ are the lattice sites and L is the system size; ε is coupling strength in space; $f(x_n(i))$ is the local dynamical function that has been chosen as the first-order reflection in Eq. (6).

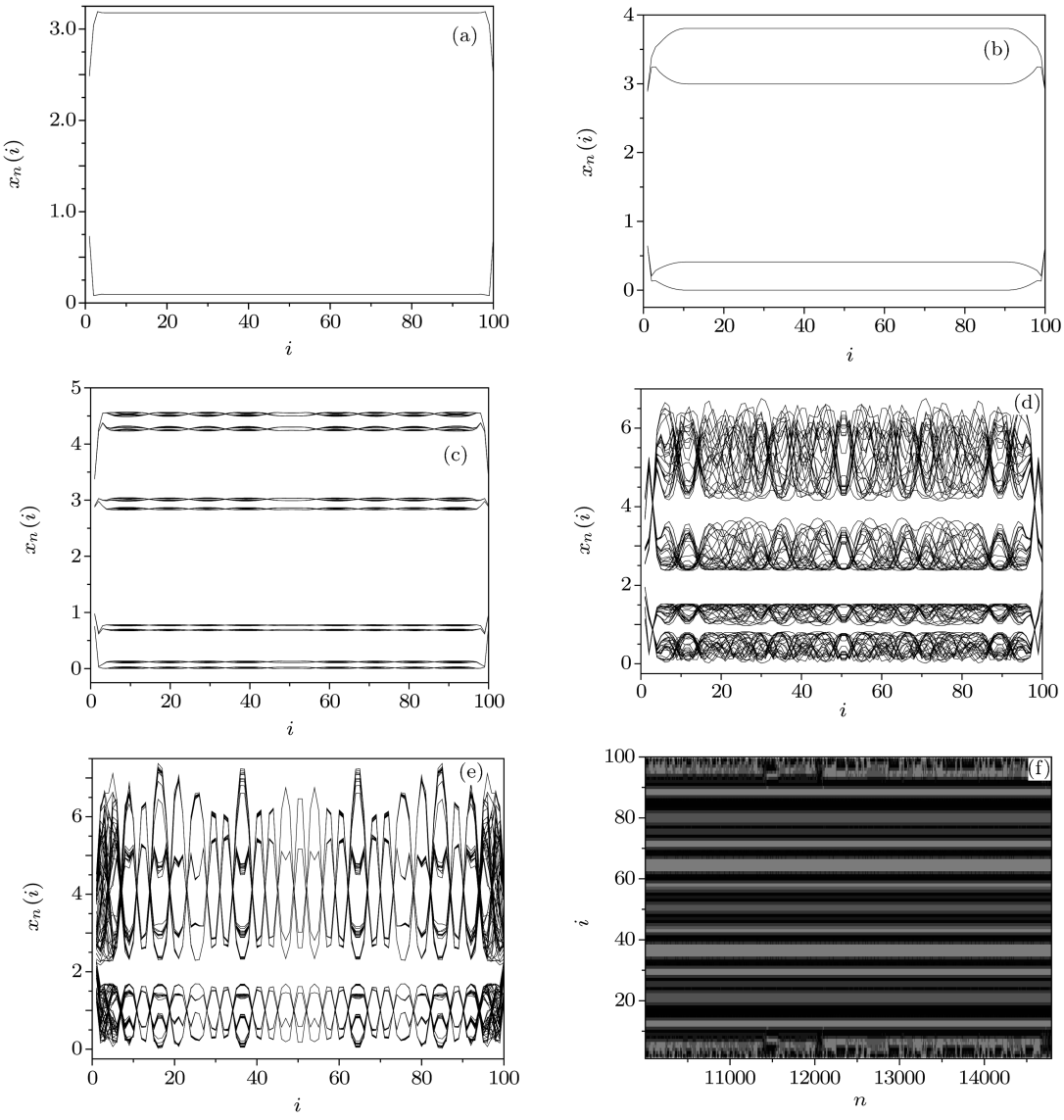


Fig. 3. Frozen random pattern for the one-dimensional SCPCS (7) after the 10000 itreations of transients with $L = 100$, $\varepsilon = 0.3$, and $B = 3.0$. (a) space–amplitude plot with $A = 2.2$, (b) space–amplitude plot with $A = 2.5$, (c) space–amplitude plot with $A = 3.0$, (d) space–amplitude plot with $A = 4.5$, (e) space–amplitude plot with $A = 5.0$, (f) space–time diagram with $A = 5.0$.

The system parameters are $B = 3.0$ and $L = 100$; the initial conditions are $x_0(i) = 0.2$, and the boundary conditions are $x_n(0) = x_n(L+1) = 0$. We solve the SCPCS (7) numerically and obtain various kinds of the patterns which are the same as the coupled logistic lattices.[2] The frozen random pattern is shown in Fig. 3. As $A = 2.2$ and $A = 2.5$, the phase-conjugate resonator appears in period-2 and period-4 as shown in Fig. 2(a). The SCPCS (7) shows the period-doubling in space–amplitude plot in Figs. 3(a) and 3(b). Amplitudes $x_n(i)$'s are overplayed for 100 time steps after the 10000 iterations of transients. Space–amplitude plots are shown in Figs. 3(c) and 3(d). Every 8th time, the plot changes from 0 to 600 after the 10000 iterations of transients. After doubling period several times, the system exhibits a chaotic behaviour in a large domain with $A = 5.0$ in Figs. 3(e) and 3(f).

Some examples of the pattern selection are shown in Fig. 4. As the system parameter A increases and the coupled strength ε is fixed, the space–amplitudes in some special sizes decrease in Figs. 4(a) and 4(b) or 4(c) and 4(d). As the system parameter A is fixed and the coupled strength ε increases, the chaotic behaviour is clearly shown in large domains in Figs. 4(a) and 4(c), while the chaotic motion is confined in small domains in Figs. 4(b) and 4(d).

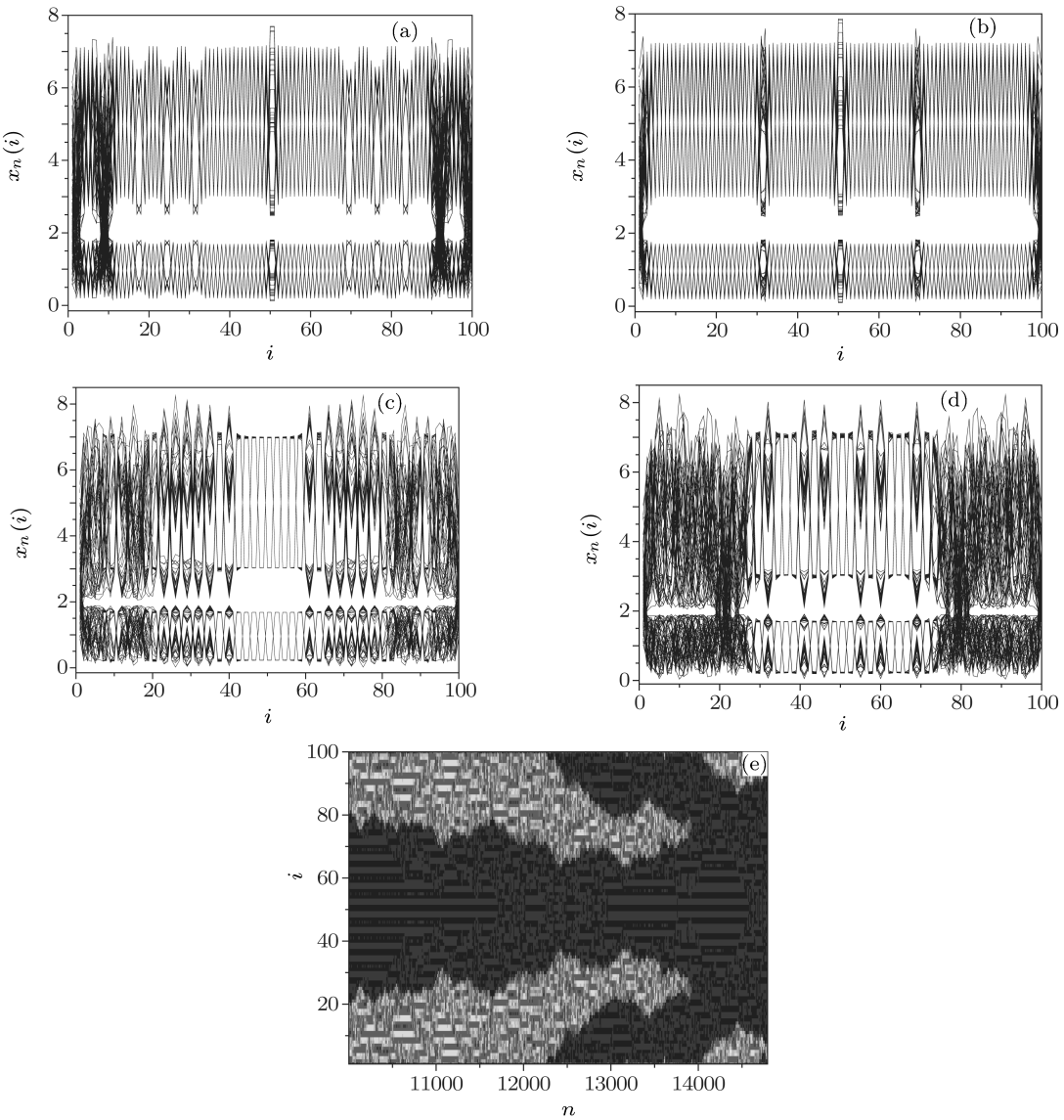


Fig. 4. Pattern selection for the one-dimensional SCPCS (7) after the 10000 itreations of transients with $L = 100$ and $B = 3.0$. (a) space–amplitude plot with $A = 5.60$ and $\varepsilon = 0.1$; (b) space–amplitude plot with $A = 5.65$ and $\varepsilon = 0.1$; (c) space–amplitude plot with $A = 5.60$ and $\varepsilon = 0.2$; (d) space–amplitude plot with $A = 5.65$ and $\varepsilon = 0.2$; (e) space–time diagram with $A = 5.65$ and $\varepsilon = 0.2$.

The selection occurring is in favour of a simple temporal motion. The diffusion term has the tendency to produce the homogeneity in space, while the chaotic motion makes the system inhomogeneous. The two tendencies conflict with each other. The conflict leads to the splitting of a large domain. After the pattern selection, the pattern of domains is fixed and does not move in space.

As the parameter increases further, the domain boundaries start to move. The remarkable point represents the existence of localised chaos as a defect in Fig. 5(a). The defects are localised in space and its shape changes chaotically in time and moves randomly around the space in Fig. 5(b).

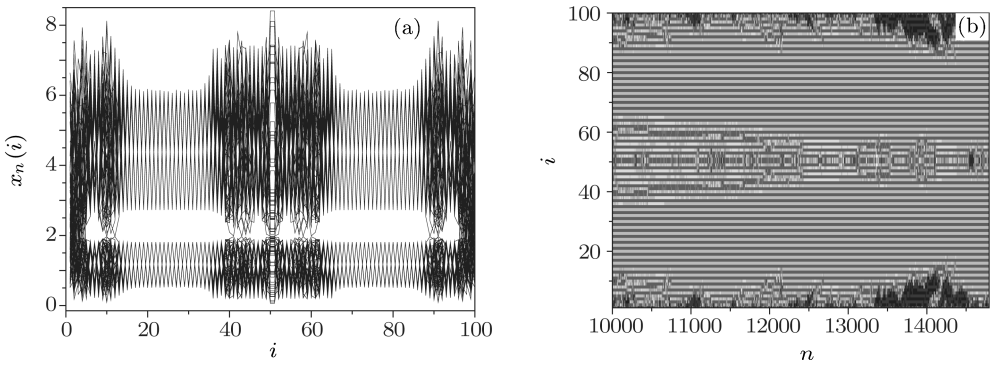


Fig. 5. Defect chaotic diffusion for the one-dimensional SCPCS (7) after the 10000 itreations of transients with $A = 5.836$, $B = 3.0$, $\varepsilon = 0.1$, and $L = 100$. (a) Space–amplitude plot, (b) space–time diagram.

As parameter A increases, the chaotic motion that makes the system inhomogeneous becomes stronger than the diffusion process. The chaotic motion in space develops into the defect turbulence in Fig. 6. If the coupling is larger, the selected pattern is not unique. There are intermittent bursts with the increase of the parameter A. The burst arises from the mismatch of phase and has larger structures than a chaotic defect in Fig. 6. As to the conflict between the ordering by diffusion and inhomogeneous by local chaos, the turbulence has fully developed as shown in Fig. 7.

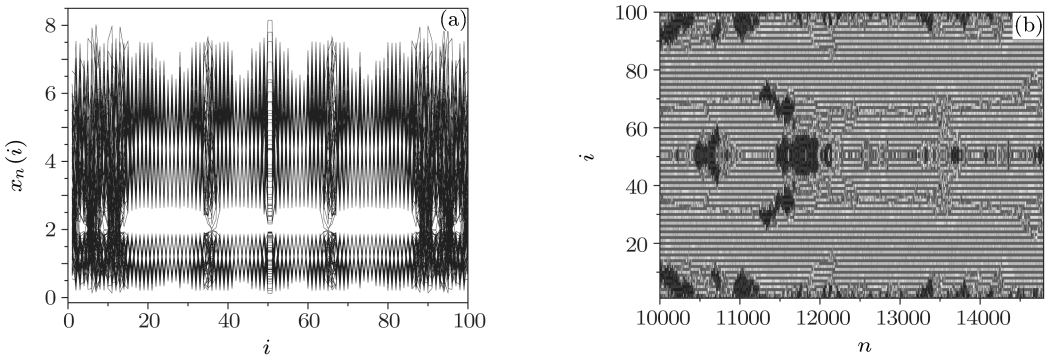


Fig. 6. Defect turbulences for one-dimensional SCPCS (7) after the 10000 itreations of transients with $A = 5.95$, $B = 3.0$, $\varepsilon = 0.1$, and $L = 100$. (a) space–amplitude plot, (b) space–time diagram.

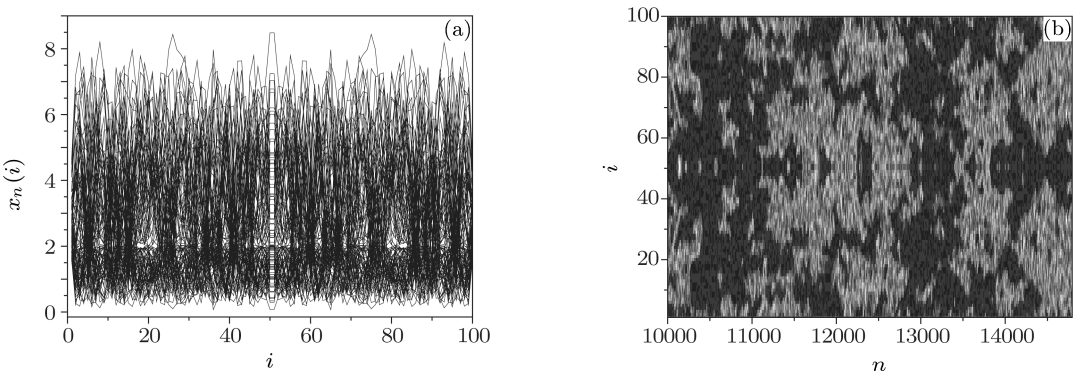


Fig. 7. Fully developed turbulences for one-dimensional SCPCS (7) after the 10000 iterations of transients with $A = 6.0$, $B = 3.0$, $\varepsilon = 0.3$, and $L = 100$. (a) space–amplitude plot, (b) space–time diagram.

3.2. Two-dimensional coupled map phase-conjugate system

Two-dimensional CML follows the general form as follows:[2]

$$x_{n+1}(i,j) = (1-\varepsilon)f(x_n(i,j)) + \frac{\varepsilon}{4}(f(x_n(i+1,j)) + f(x_n(i-1,j)) + f(x_n(i,j+1)) + f(x_n(i,j-1))), \tag{8}$$

where $n = 1, 2, \ldots N$ are the discrete time steps; $i, j = 1, 2, \ldots L$ are the two-dimensional lattice sites and L is the system size; ε is the coupling strength in space, and the local dynamical function $f(x_n(i,j))$is chosen from Eq. (6). The system parameters are $A = 6$, $B = 3$, and the coupling strength is $\varepsilon = 0.03$. Under the initial conditions there are random numbers appearing in the interval [0,1], the boundary conditions are $x_n(0,j) = x_n(i,L+1) = x_n(i,0) = x_n(L+1,i) = 0$. And the system length L is 100. We solve Eq. (8) numerically with the increase of the iteration n. The results are shown in Fig. 8. The homogeneous symmetric states induce symmetry breaking from four corners and the boundaries with the increase of the iteration n. As the iteration increases further, the patterns evolving around the boundaries induce more and more defective states in four corners. The patterns finally lead to spatiotemporal chaos.

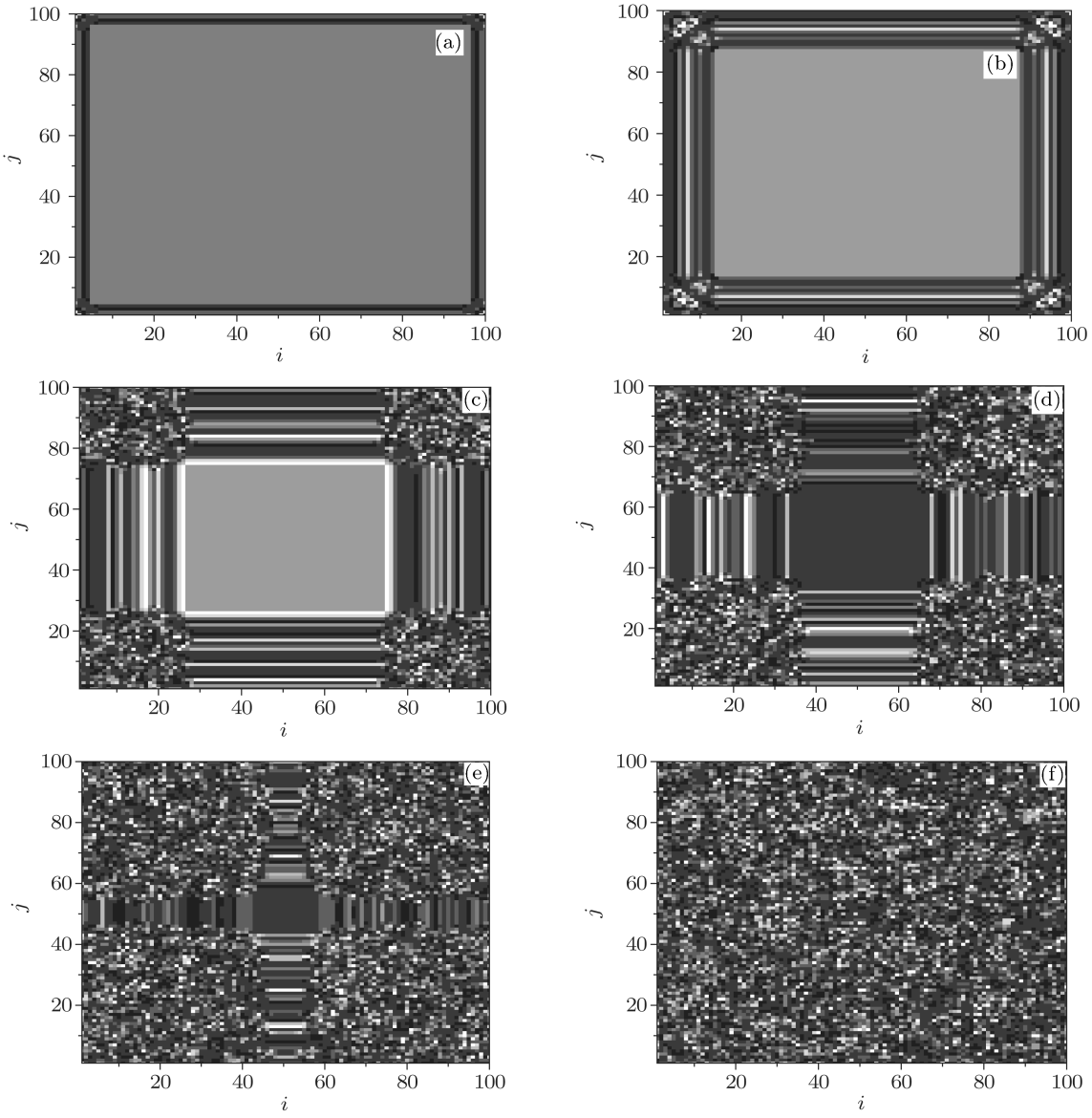


Fig. 8. Space–time diagram for two-dimensional SCPCS (8) with $A = 6$, $B = 3$, $\varepsilon = 0.03$, and $L = 100$. The homogeneous symmetric states evolve into the defective states and spatiotemporal chaos with different iterations. (a) $n = 40$, (b) $n = 80$, (c) $n = 150$, (d) $n = 200$, (e) $n = 250$, (f) $n = 300$.

4. Conclusion

Our numerical simulations demonstrate that the various patterns from the period doubling of kink–antikinks in space, the chaotic behaviours in some domains to the full turbulence are obtained with the change of the system parameters in one-dimensional SCPCS. The patterns evolve from the homogenous states and the symmetry breaking in space to the spatiotemporal chaos with the increase of the iteration time in a two-dimensional SCPCS. The results show that the most unstable modes are influenced by boundaries. Dynamic behaviours depend on the boundary condition, the initial condition and the parameters of the system.

References

[1] Kaneko K 1989 *Physica* D **34** 1
[2] Kaneko K 1989 *Physica* D **37** 60
[3] Willeboordse F H 1992 *Chaos, Solitons and Fractals* **2** 609
[4] Willeboordse F H 1993 *Phys. Rev.* E **47** 1419
[5] Kuramoto Y and Nakao H 1996 *Phys. Rev. Lett.* **76** 4352
[6] Löcher M, Johnson G A and Hunt E R 1997 *Chaos, Solitons and Fractals* **8** 1523
[7] Ouchi N B and Kaneko K 2000 *Chaos* **10** 359
[8] Qin W X and Qian D B 2000 *Chaos, Solitons and Fractals* **11** 2305
[9] Liu Z R and Luo J G 2006 *Chaos, Solitons and Fractals* **30** 1198
[10] Willeboordse F H 2003 *Chaos* **13** 533
[11] Luo X S and Fang J Q 2000 *Chin. Phys.* **9** 333
[12] Yue L J and Shen K 2005 *Chin. Phys.* **14** 1760
[13] Bo B C, Kang Z S, Xu J P and Hu W 2009 *Acta Phys. Sin.* **58** 1420 (in Chinese)
[14] Zhang X and Shen K 2000 *Proc. SPIE* **4225** 216
[15] Yue L J and Shen K 2004 *Proc. SPIE* **5646** 117
[16] Wright E M, Meystre P and Firth W J 1984 *Opt. Commun.* **51** 428
[17] Reiner G, Meystre P and Wright E M 1985 *J. Opt. Am.* B **2** 982
[18] Kwong S K and Yariv A 1986 *J. Opt. Soc. Am.* A **3** 157
[19] Belic M R and Stojkov P 1990 *Optical and Quantum Electronics* **22** 157
[20] Geddes J B, Lega J and Moloney J V 1994 *Chaos, Solitons and Fractals* **4** 1261
[21] Yue L J, Shen K and Xu M Q 2007 *Acta Phys. Sin.* **56** 4378 (in Chinese)